Comparison of secondary organic aerosol formation from toluene on initially wet and dry ammonium sulfate particles at moderate relative humidity

Tengyu Liu[1], Dan Dan Huang[1], Zijun Li[2], Qianyun Liu[3], ManNin Chan[2,4], and Chak K. Chan[1,*]

1. School of Energy and Environment, City University of Hong Kong, Hong Kong, China
2. Earth System Science Programme, The Chinese University of Hong Kong, Hong Kong, China
3. Division of Environment and Sustainability, Hong Kong University of Science and Technology, Hong Kong, China
4. The Institute of Environment, Energy and Sustainability, The Chinese University of Hong Kong, Hong Kong, China

*Corresponding author:

Chak K. Chan

School of Energy and Environment, City University of Hong Kong, China

Tel: +852-34425593

Email: Chak.K.Chan@cityu.edu.hk

Abstract

The formation of secondary organic aerosol (SOA) has been widely studied in the presence of dry seed particles at low relative humidity (RH). At higher RH, initially dry seed particles can exist as wet particles due to water uptake by the seeds as well as the SOA. Here, we investigated the formation of SOA from the photooxidation of toluene using an oxidation flow reactor in the absence of NO_x under a range of OH exposures on initially wet or dry ammonium sulfate (AS) seed particles at an RH of 68%. The ratio of the SOA yield on wet AS seeds to that on dry AS seeds, the relative SOA yield, decreased from 1.31±0.02 at an OH exposure of 4.66×10^{10} molecules cm^{-3} s to 1.01±0.01 at an OH exposure of 5.28×10^{11} molecules cm^{-3} s. This decrease may be due to the early deliquescence of initially dry AS seeds after coated by highly oxidized toluene-derived SOA. SOA formation lowered the deliquescence RH of AS and resulted in the uptake of water by both AS and SOA. Hence the initially dry AS seeds contained aerosol liquid water (ALW) soon after SOA formed and the SOA yield and ALW approached those of the initially wet AS seeds as OH exposure and ALW increased, especially at high OH exposure. However, a higher oxidation state of the SOA on initially wet AS seeds than that on dry AS seeds was observed at all levels of OH exposure. The difference in mass fractions of *m/z* 29, 43 and 44 of SOA mass spectra, obtained using an aerosol mass spectrometer (AMS), indicated that SOA formed on initially wet seeds may be enriched in earlier-generation products containing carbonyl functional groups at low OH exposures and later-generation products containing acidic functional groups at high exposures. Our results suggest that

inorganic dry seeds become at least partially deliquesced particles during SOA formation and hence ALW is inevitably involved in the SOA formation at moderate RH. More laboratory experiments conducted with a wide variety of SOA precursors and inorganic seeds under different NO_x and RH conditions are warranted.

1. Introduction

Secondary organic aerosol (SOA) is an important component of atmospheric particulate matter, which influences air quality, climate and human health (Hallquist et al., 2009). SOA is mainly formed via the oxidation of volatile organic compounds (VOCs), followed by partitioning to the condensed phase. Traditional atmospheric chemical transport models largely underestimate the levels of SOA (de Gouw et al., 2005; Volkamer et al., 2006; Hodzic et al., 2010) and the degree of oxidation (Rudich et al., 2007; Ng et al., 2010). The updated models incorporating the volatility basis set (VBS) formalism (Donahue et al., 2006) can better predict the observed SOA, but SOA formation still remains under-constrained (Shrivastava et al., 2011; Tsigaridis et al., 2014; Hayes et al., 2015; Ma et al., 2017). SOA yields in atmospheric chemical transport models are obtained from smog chamber experiments using dry seed particles (Barsanti et al., 2013; Mahmud and Barsanti, 2013) under dry conditions. Yet, atmospheric relative humidity is often sufficiently high that aerosols often contain aerosol liquid water (ALW) due to their hygroscopic properties (Liao and Seinfeld, 2005; Lee and Adams, 2010; Guo et al., 2015; Nguyen et al., 2016). The presence of ALW in aerosols may enhance SOA formation by facilitating the partitioning of semivolatile organic compounds and the uptake of water-soluble gases through aqueous-phase reactions (Hennigan et al., 2008; Lim et al., 2010; Ervens et al., 2011; Lee et al., 2011; Sareen et al., 2017). ALW may also promote photodegradation of dissolved SOA (Romonosky et al., 2014). Therefore, SOA formation under atmospherically relevant relative humidity needs to be better constrained in

atmospheric chemical transport models by incorporating ALW. In addition, understanding water uptake of SOA is important for estimating its loss by wet deposition, which is not well constrained.

Aromatic hydrocarbons constitute a large fraction of the total non-methane hydrocarbons in the urban atmosphere (Calvert et al., 2002) and account for a significant fraction of SOA in urban areas (Ding et al., 2012; Zhao et al., 2017). Toluene is the most abundant aromatic hydrocarbon (Calvert et al., 2002; Zhang et al., 2016) and SOA yields from the photooxidation of toluene on dry or wet ammonium sulfate (AS) seeds has been studied by varying the RH in smog chambers. Kamens et al. (2011) observed higher yields of SOA from toluene at higher RHs. They attributed this increase to the initially wet seed particles. On the other hand, Edney et al. (2000) reported that wet seeds had no effect on the SOA yields of toluene compared with dry seeds. In these studies, different RHs used for dry and wet seeds experiments may influence the gas-phase chemistry and complicate the comparison of SOA formation.

SOA formation on initially dry and wet AS seeds has been compared using oxidation flow reactors at same RHs (Wong et al., 2015; Faust et al., 2017). Faust et al. (2017) found a 19% enhancement in the SOA yield of toluene on wet AS seeds over that on dry AS seeds at 70% RH. However, at such high RH, the initially dry and water-free AS seed particles can uptake water upon SOA formation because SOA themselves can be hygroscopic and they can also lower the deliquescence RH of the AS seeds (Takahama et al., 2007; Smith et al., 2011, 2012, 2013). The potential influence of SOA formation on the physical state of the initially dry seeds as well as and the overall water

uptake by the aged particles was not explicitly discussed. In addition, the hydroxyl radicals (OH) exposure in Faust et al. (2017) was approximately 2×10^{11} molecules cm^{-3} s, equivalent to about 1.5 days of oxidation in the atmosphere assuming an ambient OH concentration of 1.5×10^{6} molecules cm^{-3} (Mao et al., 2009). Atmospheric particles can undergo oxidation for as long as 1-2 weeks (Balkanski et al., 1993).

In this study, SOA formation from the photooxidation of toluene was investigated in an oxidation flow reactor at an RH of 68% under a wide range of OH exposures using initially wet or dry AS seed particles. The yields and composition of SOA as well as the estimated ALW contents for the initially wet and dry seeds are compared. We found that as OH exposure increased, the SOA yield and ALW of the initially dry seeds approached those of the initially wet seeds while the wet seeds yielded SOA of a higher degree of oxidation than the dry seeds did at all exposure levels.

2. Materials and methods

2.1 Generation of seed particles

A schematic of the experimental setup, similar to that used in Wong et al. (2015) and Faust et al. (2017), is shown in Fig. 1. AS seed particles were generated from an aqueous AS solution (Sigma-Aldrich) using an atomizer (TSI 3076, TSI Inc., USA). In experiments using dry seeds, the atomized aqueous AS droplets passed through a silica gel diffusion dryer so that the RH was reduced to less than 30% at which AS effloresced, while in experiments using wet seeds, they bypassed the diffusion dryer. The dry or wet seed particles then entered and mixed with a humidified $N_2/O_2/O_3$ flow in an oxidation flow reactor. The RH in the flow reactor was at 68%, which lies between the

efflorescence and deliquescence RH of AS (Seinfeld and Pandis, 2006), so that the seed particles remained in their original phase with the wet particles containing ~18.6 μg m^{-3} ALW (see Section 2.4) and the dry particles anhydrous before reaction started. Hereafter, the experiments using initially wet and dry AS seed particles are simplified as wet and dry AS seeds, respectively. "Wet" and "dry" refer to the initial state of the seed particles before SOA formation.

When atomizing a given AS solution, the diameter of wet AS droplets is much larger than that of dry AS particles due to the water uptake of AS (Chan et al., 1992), resulting in a larger surface area of seed particles. Previous studies have demonstrated that a large surface area of seed particles may increase the SOA yields by reducing the wall loss of organic vapors (Matsunaga and Ziemman, 2010, Zhang et al., 2014, 2015; Huang et al., 2016; Krechmer et al., 2016). To obtain seed particles of comparable surface areas, we atomized 0.013 mM and 0.015 mM of the AS solution for wet and dry AS seeds, respectively. As shown in Fig. S1, the surface area distribution of initially wet AS seeds was similar to that of initially dry AS seeds. Because of the difference in AS concentration between the stock solutions used, wet AS seeds had a mean diameter of 88 nm and were slightly smaller than dry AS seeds which had a mean diameter of 102 nm. The total surface area of wet AS seeds was 21% larger than that of dry AS seeds. The mass loading of wet and dry AS seeds was 31.0 and 24.2 μg m^{-3}, respectively.

2.2 Oxidation flow reactor

SOA formation from the photooxidation of toluene in the absence of NO_x on initially dry or wet seeds was investigated in a potential aerosol mass (PAM) oxidation flow

reactor, which has been described in detail elsewhere (Kang et al., 2007, 2011; Lambe et al., 2011a, 2015; Liu et al., 2017). Briefly, a PAM chamber is a continuous oxidation flow reactor using high and controlled levels of oxidants to oxidize gaseous precursors to produce SOA. The chamber used in this study had a volume of approximately 19 L (length 60 cm, diameter 20 cm). The total flow rate in the PAM chamber was set at 3 L min^{-1} using mass flow controllers, resulting in a residence time of approximately 380 s. The RH and temperature of the PAM outflow were measured continuously (HMP 110, Vaisala Inc, Finland) and stabilized at approximately 68% and 20 ºC, respectively. High OH exposures were realized through the photolysis of ozone irradiated by a UV lamp (λ = 254 nm) in the presence of water vapor. Ozone was produced by an ozone generator (1000BT-12, ENALY, Japan) via the irradiation of pure O_2. The OH concentration was adjusted by varying the concentration of ozone in the PAM chamber from 0.4 ppm to 4.3 ppm. The corresponding upper limit of OH exposure at these operating conditions ranged from 0.47×10^{11} molecules cm^{-3} s to 5.28×10^{11} molecules cm^{-3} s, equivalent to 0.36 to 4.08 days of atmospheric oxidation assuming an ambient OH concentration of 1.5×10^{6} molecules cm^{-3} (Mao et al., 2009). The upper limit of OH exposure was determined by measuring the decay of SO_2 (Model T100, TAPI Inc., USA) in the absence of toluene, following procedures described elsewhere (Kang et al., 2007; Lambe et al., 2011a). The reduction in OH exposure due to the addition of toluene was estimated to range from 15% at the highest OH exposure to 25% at the lowest OH exposure, using the method of Peng et al. (2016). Peng et al. (2016) found that non-OH chemistry, including photolysis at λ = 254 nm and reactions with $O(^1D)$, $O(^3P)$ and O_3,

may play an important role in oxidation flow reactors. In this study, the PAM reactor was operated at water vapor mixing ratios above 0.5% and external OH reactivity below 20 s^{-1}. Non-OH chemistry is expected to play a negligible role under these conditions (Peng et al., 2016).

Before and after each experiment, the PAM reactor was cleaned under an OH exposure of ~1×10^{12} molecules cm^{-3} s until the mass concentration of background particles dropped below 3 μg m^{-3}. After characterizing dry or wet AS seed particles for half an hour, the UV lamp was turned on to oxidize the background gases at five different OH levels to measure the concentrations of background organics. A toluene mixture (29.6 ppm in nitrogen) with a flow rate of 0.013 L min^{-1} was then introduced to initiate SOA formation. The initial concentration of toluene in the PAM reactor was approximately 138 ppb. The reacted and final concentrations of toluene were calculated from the OH exposure and the rate constant of the reaction between toluene and OH (Atkinson and Arey, 2003) (Table 1). The flow and light conditions were the same for initially wet and dry seeds. Therefore, the quantification of toluene would not introduce uncertainties to the relative SOA yields described in Section 3.1 as the initial concentrations of toluene and OH exposures were the same for both cases. SOA was measured for at least an hour with a step-wise increase in the five OH levels.

2.3 Characterization of non-refractory components

The AS/SOA mixed particles were characterized for the chemical composition of non-refractory components including organics, sulfate and ammonium as well as the elemental ratios of organics using a high-resolution time-of-flight aerosol mass

spectrometer (hereafter AMS, Aerodyne Research Incorporated, USA) (DeCarlo et al., 2006). The instrument was operated in the high sensitivity V-mode and the high resolution W-mode alternating every one minute. The toolkit Squirrel 1.57I and Pika 1.16I were used to analyze the AMS data. The molar ratios of hydrogen to carbon (H:C) and oxygen to carbon (O:C) were determined using the Aiken method (Aiken et al., 2007, 2008). The ionization efficiency of the AMS was calibrated using 300 nm ammonium nitrate particles. The particle-free matrix air, obtained by passing the air flow from the PAM reactor through a HEPA filter, was measured for at least 20 min before each experiment to determine the signals from major gases.

The collection efficiency (CE) of an AMS is dependent on the chemical composition and acidity as well as the phase state of particles (Matthew et al., 2008; Middlebrook et al., 2012). Matthew et al. (2008) found that the CE for solid particles thickly coated with liquid organics was 100%. In this study, experiments were conducted at an RH of 68%, exceeding the RH threshold for the semisolid-to-liquid phase transition for toluene-derived SOA (Bateman et al., 2015; Song et al., 2016). The toluene-derived SOA in these experiments was therefore liquid-like. The unimodal size distributions of particle numbers show the SOA formation on AS seed particles without much nucleation mode particles (Fig. S2). A CE of 1 was used for processing all AMS data since the AS seed particles were coated by liquid SOA. The adoption of this CE value was supported by that the concentration of sulfate measured with the AMS varied by less than 5% of the average mass of sulfate after coated by SOA for both wet and dry AS seeds conditions. For the quantification of SOA, the contribution from

background organic aerosols was subtracted from the total organic aerosols. The ratio of SOA mass to background organic mass ranged from 7 to 59, indicating that the contribution from background organics was negligible. Aerosol particles typically pass through a silica gel diffusion dryer to remove ALW before they are measured by AMS. However, this may lead to some losses of semivolatile organics through reversible partitioning (Wong et al., 2015; Faust et al., 2016). In this study, the AS/SOA mixed particles stream passed through and bypassed a diffusion dryer alternately before they were measured by AMS. Overall less than 8% of SOA were lost for wet and dry AS seeds after passing the diffusion dryer (Fig. S3), possibly due to reversible partitioning of the SVOCs. In this paper, the data reported are those bypassing the diffusion dryer.

A scanning mobility particle sizer (SMPS, TSI Incorporated, USA, classifier model 3082, CPC model 3775) was used to measure particle number concentrations and size distributions. Particle size ranged from 15 nm to 661 nm.

To evaluate the influence of seed surface area on SOA formation, we conducted another experiment at OH exposure of 0.47×10^{11} molecules cm^{-3} s with 50% of the seed surface area used in the wet AS experiment. The difference in SOA concentration was approximately 1% between these two experiments. Hence the 20% difference in seed surface area as well as the difference in mass loadings between wet and dry AS particles cannot account for the difference in SOA yield to be discussed below.

2.4 Estimation of aerosol liquid water (ALW) content

The ALW content of the initially dry AS was zero. However, as reactions proceed, SOA themselves can uptake water and also lower the deliquescence RH of AS, leading to

water uptake by AS and some fractions of AS in aqueous phase. The ALW contents of AS (ALW_{AS}) and toluene-derived SOA (ALW_{SOA}) were estimated from the following equations (Kreidenweis et al., 2008):

$$ALW_{AS} = V_{AS}\kappa_{AS} f \frac{\alpha_w}{1-\alpha_w}\rho_w \quad (1)$$

$$ALW_{SOA} = V_{SOA}\kappa_{SOA} \frac{\alpha_w}{1-\alpha_w}\rho_w \quad (2)$$

where V_{AS} and V_{SOA} represent the volume concentrations of dry AS and SOA particles, κ_{AS} is the hygroscopicity parameter of AS particles obtained from Kreidenweis et al. (2008), κ_{SOA} is the hygroscopicity parameter of toluene-derived SOA calculated using the linear correlation between κ_{SOA} and the O:C ratios of SOA proposed by Lambe et al. (2011b), the term f is the fraction of AS particles that dissolved, α_w is the water activity and ρ_w is the density of water (1.0 g cm^{-3}). Here, α_w was assumed to be equivalent to RH/100 for simplicity. The volume concentrations of dry AS and SOA particles were estimated from the measured mass concentration of AS and SOA assuming their respective particle densities to be 1.77 g cm^{-3} and 1.4 g cm^{-3} (Ng et al., 2007).

For the initially wet AS seeds, all AS particles were completely aqueous and therefore f = 1. For the initially dry AS seeds, before reactions, the AS particles were completely dry and f = 0. After reactions, the AS particles became partially or entirely deliquesced upon the formation of toluene-derived SOA. The dissolved fraction of AS particles was regulated by the liquidus curve of the deliquescence relative humidity (DRH(ε)) of AS particles coated with toluene-derived SOA (Smith et al., 2013):

$$f = \begin{cases} \dfrac{\varepsilon(1-\varepsilon_D)}{\varepsilon_D(1-\varepsilon)} & for\ \varepsilon < \varepsilon_D \\ 1 \quad for \quad \varepsilon \geq \varepsilon_D \end{cases} \tag{3}$$

The term ε is the volume fraction of SOA (Table 1). The term ε_D, representing the volume fraction of organics at which the mixture of SOA and AS particles deliquesced at an RH of 68%, was estimated to be 0.75 based on the liquidus curve.

3. Results and discussion

3.1 SOA yields

Figure 2a shows SOA yields from the photooxidation of toluene on initially wet and dry AS seed particles as a function of OH exposure. The SOA yield was calculated as the SOA mass divided by the mass of reacted toluene. The uncertainty in the SOA yields simply reflected the standard derivation when averaging the SOA mass. In both cases, SOA yields first exhibited an increase, followed by a decrease as the level of OH exposure increased. This trend may be due to the transition of functionalization reactions to fragmentation ones (Kroll et al., 2009; Lambe et al., 2011a). Previous oxidation flow reactor studies suggest that gas-phase chemistry dominates over heterogeneous OH oxidation at OH levels below 1.0×10^{12} molecules cm^{-3} s (Ortega et al., 2016; Palm et al., 2016). In this study, the highest OH exposure was 5.28×10^{11} molecules cm^{-3} s and heterogeneous oxidation of SOA may not play an important role in reducing the mass of SOA, although we cannot exclude that it plays a role. In addition, glyoxal is an important oxidation product of toluene (Kamens et al., 2011). The reactive uptake of glyoxal has been demonstrated to enhance rather than reduce the SOA mass (Liggio et al., 2005a). The SOA yields for dry and wet AS seeds were 0.18–0.31 and

0.22–0.36, respectively, significantly higher than the value of 0.0059 observed in an oxidation flow reactor under comparable conditions (Faust et al., 2017) and the value of 0.09 obtained in another PAM chamber at 30% RH in the absence of seed particles (Kang et al., 2007). Faust et al. (2017) attributed their significantly lower yields than typical literature values of 0.09–0.30 (Lambe et al., 2011a; Ng et al., 2007) to the wall loss of particles and the fragmentation of organics in their flow reactor. On the other hand, the SOA yields we obtained are lower than the values of 0.30–0.37 from smog chamber experiments conducted at a similar temperature, SOA mass loading and OH exposure but a lower RH with dry AS seeds (Ng et al., 2007; Hildebrandt et al., 2009). Note that the wall loss of particles was not corrected in this study, so the SOA yields may be underestimated. As wet and dry AS seeds in this study had similar particle number size distributions, the wall loss of particles would not affect the comparison of SOA yield between wet and dry AS seeds.

As shown in Fig. 2a, a higher SOA yield was observed for wet AS seeds than for dry AS seeds at the same OH exposure and the difference in SOA yield decreased as the OH exposure increased. The ratio of SOA yields on wet AS seeds to those on dry AS seeds, the relative SOA yield, was 1.31±0.02 at an OH exposure of 0.47×10^{11} molecules cm^{-3} s but decreased to 1.01±0.01 when the OH exposure was increased to 5.28×10^{11} molecules cm^{-3} s (Fig. 2b). These ratios are comparable to the 1.19±0.05 observed by Faust et al. (2017) at an OH exposure of approximately 2.0×10^{11} molecules cm^{-3} s.

The formation of SOA on initially dry AS particles may alter the deliquescence

285 relative humidity (DRH) of AS particles. Smith et al. (2013) found that when coated
286 with toluene-derived SOA, the DRH of AS particles decreased from 80% to 58% as the
287 organic volume fraction increased from 0 to 0.8. Therefore, coating AS particles with
288 toluene-derived SOA can change the physical state of initially dry AS seeds and
289 increase the content of $ALW_{AS,\ dry}$. As shown in Fig. 3a, after reactions, the mass
290 concentrations of ALW_{tot} (= ALW_{SOA} + ALW_{AS}) and ALW_{SOA} increased for both wet
291 and dry seeds as the OH exposure increased. The uncertainties for ALW_{SOA} and ALW_{AS}
292 were 22% and less than 3%, respectively. They reflect the uncertainties in κ and volume
293 concentrations of AS and SOA. The increase in $ALW_{tot,\ wet}$ was due to the increase in
294 $ALW_{SOA,\ wet}$ while the increase in $ALW_{tot,\ dry}$ was driven by the increase in $ALW_{AS,\ dry}$ at
295 lower OH exposure and by $ALW_{SOA,\ dry}$ at higher OH exposures. At OH exposure of
296 0.47×10^{11} molecules cm^{-3} s, $ALW_{AS,\ dry}$ increased from 0 to 6.2 μg m^{-3} after reactions
297 due to the partial deliquescence (f=0.43) of the originally dry AS particles after SOA
298 formation. The difference in $ALW_{AS,\ dry}$ and $ALW_{AS,\ wet}$ narrowed and the ALW_{total} of
299 initially dry AS seeds partially resembled those of the wet ones. At OH exposure
300 between 1.66×10^{11} and 5.28×10^{11} molecules cm^{-3} s, the total final organic volume
301 fraction increased to approximately 0.8 and the initially dry AS particles entirely
302 deliquesced after reactions. Based on the reported SOA yield, initial toluene
303 concentration, OH exposure and assumed concentrations of AS seeds (~10-40 μg m^{-3})
304 in Faust et al. (2017), we estimated that an upper limit of 48% of the initially dry AS
305 seeds has deliquesced in their study. Similar to this study, SOA coatings on seed
306 particles may change the physical state of initially dry seeds and lower the difference

of SOA yields between initially dry and wet seeds experiments.

The hydrophilic products can partition more readily into initially wet AS seeds than dry seeds and partially account for the difference in SOA yields. For example, as one of the important oxidation products, glyoxal was estimated to have an effective Henry's law constant of 4.52×10^{8} m atm^{-1} for our initially wet AS seeds due to the "salting-in" effect (Kampf et al., 2013), approximately 3 orders of magnitude higher than that in pure water (Ip et al., 2009). The uptake rate constant of glyoxal can be calculated as (γvA)/4, where γ is the uptake coefficient, v is the gas-phase velocity of glyoxal, and A is the total surface area of AS seeds. The uptake rate constant is 4.5×10^{-4} s^{-1} for initially wet seeds with $\gamma = 2.4\times10^{-3}$ estimated from glyoxal uptake in AS seeds at 68% RH (Liggio et al., 2005b). The average gas-phase glyoxal concentration was modeled to be 4.3 ppb at OH exposure of 0.47×10^{11} molecules cm^{-3} s using the Master Chemical Mechanism v 3.3.1 (Jenkin et al., 2003; Bloss et al., 2005), which would result in approximately 1.6 μg m^{-3} of glyoxal in particle phase for initially wet AS seeds. If the particle-phase concentration of glyoxal was assumed to be 0 for initially dry AS seeds, the enhanced partitioning of glyoxal alone would account for 24.5% of the mass difference of SOA. Note that other hydrophilic products were not included in this calculation. This analysis suggests that the enhanced partitioning of hydrophilic products may play an important role in the difference of SOA yields at low OH exposures. As discussed above, the initially dry AS seeds approached wet seeds and reduce the differences between wet and dry SOA yields at high OH exposures.

3.2 Chemical composition of SOA

Figure 4 shows the high-resolution mass spectra of SOA for initially wet and dry AS seeds at OH exposures of 0.47×10^{11} molecules cm^{-3} s and 5.28×10^{11} molecules cm^{-3} s. For both types of AS seeds, at an OH exposure of 0.47×10^{11} molecules cm^{-3} s, the most prominent peaks were *m/z* 29 and 43, followed by *m/z* 28 and 44. *m/z* 29 was dominated by ion CHO^+, a tracer for alcohols and aldehydes (Lee et al., 2012). The *m/z* 28 and *m/z* 44 signals, respectively dominated by CO^+ and CO_2^+, are tracers for organic acids (Ng et al., 2010). At the OH exposure of 5.28×10^{11} molecules cm^{-3} s, the dominant peaks were *m/z* 28 and 44, followed by *m/z* 29 and 43. The increase of mass fractions of the oxygen-containing ions in the SOA mass spectra at a relatively high OH exposure suggests the formation of more oxidized organic aerosols. On the basis of the mass fraction of ions, Fig. S4 shows that as OH exposure increased, the difference (wet minus dry) in the spectra of toluene-derived SOA changed from positive in *m/z* 29 (CHO^+) and *m/z* 43 ($C_2H_3O^+$) to *m/z* 28 (CO^+) and *m/z* 44 (CO_2^+). The increase in OH exposure resulted in a change from more alcohols or aldehydes to more organic acids in the wet seeded case when compared to the dry seeded case.

Fragments derived from the AMS data have been extensively used to infer the bulk compositions and evolution of organic aerosols (Zhang et al., 2005; Ng et al., 2010; Heald et al., 2010). Here we used the approach of Ng et al. (2010) and plotted the fractions of the total organic signal at *m/z* 43 (f_{43}) vs. *m/z* 44 (f_{44}) as well as the triangle based on the analysis of ambient AMS data (Fig. 5). Ng et al. (2010) proposed that aging would cause f_{43} and f_{44} to converge toward the triangle apex ($f_{43} = 0.02$, $f_{44} = 0.30$). For both wet and dry AS seeds, f_{43} first increased and then decreased with the increase

of OH exposure, while f_{44} increased all the time. This reversing trend of f_{43} was the result of the increase and subsequent decrease in $C_2H_3O^+$ (Fig. S5), an indicator of products containing carbonyl functional groups. The f_{43}-f_{44} plot supports our earlier assertion that as OH exposure increased, the reaction products changed from earlier-generation products containing carbonyl functional groups dominated to later-generation products containing acidic functional groups dominated. It was also observed for SOA formed from other precursors such as alkanes and naphthalene (Lambe et al., 2011b). Before the decrease in f_{43}, SOA formed on wet AS seeds had higher f_{43} and similar f_{44} to SOA formed on dry AS seeds at the same OH exposure. As OH exposure increased, SOA formed on wet AS seeds had higher f_{44} and lower f_{43} than SOA formed on dry AS seeds. In addition, as OH exposure increased, SOA formed on wet AS seeds initially had more earlier-generation products but later had more acidic later-generation products than SOA formed on dry AS seeds, likely due to the enhanced partitioning of these products on initially wet AS seeds and/or enhanced uptake of water-soluble gases through aqueous phase reactions.

Figure 6 shows the changes in H:C and O:C ratios as a function of OH exposure in a Van Krevelen diagram (Heald et al., 2010). The standard deviations for H:C and O:C values, determined for the steady-state periods, were all less than 0.01. The O:C ratios for dry and wet AS seeds were in the ranges of 0.59–0.89 and 0.63–0.95, respectively. At the same OH exposure, SOA on wet AS seeds had both higher O:C ratios and estimated average carbon oxidation state (OS_C) ($OS_C \approx 2\times O{:}C - H{:}C$) (Kroll et al., 2011) than dry AS seeds had. Fig. 6 also shows some of the identified SOA products from the

373 photooxidation of toluene (Bloss et al., 2005; Hamilton et al., 2005; Sato et al., 2007).
374 The elevated OS_C (exceeding 0.5) could only be due to the formation of highly
375 oxgenerated small acids such as pyruvic acid (OS_C = 0.67), glycolic acid (OS_C = 1),
376 formic acid (OS_C = 2), oxalic acid (OS_C = 3), malonic acid (OS_C = 1.33) and glyoxylic
377 acid (OS_C = 2). Small acids may be important products of toluene-derived SOA at high
378 OH exposures. Fisseha et al. (2004) found that small organic acids accounted for 20–
379 45% of SOA from the photooxidation of 1,3,5-trimethylbenzene. The higher OS_C at
380 high OH exposures for wet AS seeds might suggest that these small acids were more
381 abundant, likely due to their enhanced retention in the presence of ALW and/or the
382 more efficient uptake of OH radicals by wet AS seeds and further oxidation reactions
383 in aqueous phase (Ruehl et al., 2013).

384 We evaluate whether enhanced uptake of OH radicals on initially wet AS seeds
385 could explain the difference in oxygen contents, following the method of DeCarlo et al.
386 (2008). We calculated R, the ratio of the difference in oxygen of OA between the
387 initially wet and dry AS seed particles to the difference in the total number of OH
388 collisions with OA at different OH exposures. To obtain R, the uptake coefficient (γ) of
389 OH radicals was assumed to be 1 and 0.1/0.8 (lower/upper limit) for initially wet and
390 dry AS seed particles, respectively (George and Abbatt, 2000). Note that as SOA
391 formation takes place, the initially dry AS can become wet and the difference in γ
392 between initially wet and dry seeds is reduced, especially at higher OH exposures. We
393 also assumed that each collision of OH with OA resulted in the addition of one oxygen
394 atom to SOA. A value of R smaller than unity qualitatively indicates that the uptake of

OH radicals can potentially explain the differences in oxygen contents in the dry and wet experiments. Fig. S6 shows that R is larger than unity at low OH exposures and smaller than unity at high OH exposures. This analysis suggests that the enhanced OH uptake may contribute to the difference in oxygen contents between dry and wet cases at higher OH exposures. At low OH exposures, the enhanced gas-particle partitioning may dominate the difference.

The change in the slope of H:C vs O:C is consistent with the earlier analysis that the mechanism of SOA formation changed from functionalization dominated by the addition of alcohol/peroxide (Heald et al., 2010; Ng et al., 2011) at low exposures to the addition of both acid and alcohol/peroxide functional groups without fragmentation, and/or the addition of acid groups with fragmentation at high exposures.

3.3 Atmospheric implications

In this work, yields and composition of SOA formed from the photooxidation of toluene on initially wet and dry AS seeds were compared over a wide range of OH exposures, covering the transition from functionalization reactions to fragmentation reactions. We found that the ratio of SOA yield on wet AS seeds to that on dry AS seeds decreased from 1.31 to 1.01 as the OH exposure increased from 0.47×10^{11} to 5.28×10^{11} molecules cm^{-3} s. This decrease coincides with the decrease of differences in ALW between the wet and dry cases, which may be due to water uptake by SOA as well as the early deliquescence of dry AS particles as a result of SOA formation. Hence, the SOA yield and ALW of the initially dry AS seeds approached those of the initially wet AS seeds as OH exposure and ALW increased.

In addition to relatively higher SOA yields, higher O:C and OS_c of SOA derived from the photooxidation of toluene were also observed on initially wet AS seeds. Particularly, the O:C in the presence of initially wet AS seeds could be as high as 0.95. Chen et al. (2015) observed large gaps between laboratory and ambient measured O:C of OA and suggested that OA having a high O:C (> 0.6) was required to bridge these gaps. The multiphase oxidation of toluene in the presence of wet aerosols may be a pathway to contribute to this gap. However, the relative importance of such chemistry to the evolution of ambient OA remains unclear.

Our results suggest that dry seeds would quickly turn to at least partially deliquesced particles upon SOA formation under moderate RH conditions. We only studied the photooxidation of toluene in the absence of NO_x as it is still a challenge to study high-NO chemistry in oxidation flow reactors without using atmospherically irrelevant high concentrations of NO_x (Peng and Jimenez, 2017). However, the ALW may also be important to SOA formation under high NO_x conditions that preferentially form highly water-soluble products (Ervens et al., 2011). Since ambient RH is rarely at such low values that inorganic particles remain dry even after SOA formation, more laboratory and field studies are needed to elucidate the formation and evolution of OA under various NO_x conditions at moderate RH.

Acknowledgments

The work described in this paper was sponsored by the Science Technology and Innovation Committee of Shenzhen Municipality (project no. JCYJ20160401095857424). Zijun Li and ManNin Chan are supported by a Direct Grant for Research (4053159), The Chinese University of Hong Kong and a Research Grants Council grant (RGC 2191111). Chak K. Chan would like to thank the Hong Kong University of Science and Technology for the use of the AMS.

References

Aiken, A. C., DeCarlo, P. F., and Jimenez, J. L.: Elemental Analysis of Organic Species with Electron Ionization High-Resolution Mass Spectrometry, Anal. Chem., 79, 8350-8358, https://doi.org/10.1021/ac071150w, 2007.

Aiken, A. C., DeCarlo, P. F., Kroll, J. H., Worsnop, D. R., Huffman, J. A., Docherty, K. S., Ulbrich, I. M., Mohr, C., Kimmel, J. R., Sueper, D., Sun, Y., Zhang, Q., Trimborn, A., Northway, M., Ziemann, P. J., Canagaratna, M. R., Onasch, T. B., Alfarra, M. R., Prevot, A. S. H., Dommen, J., Duplissy, J., Metzger, A., Baltensperger, U., and Jimenez, J. L.: O/C and OM/OC Ratios of Primary, Secondary, and Ambient Organic Aerosols with High-Resolution Time-of-Flight Aerosol Mass Spectrometry, Environ. Sci. Technol., 42, 4478-4485, https://doi.org/10.1021/es703009q, 2008.

Atkinson, R., and Arey, J.: Atmospheric Degradation of Volatile Organic Compounds, Chem. Rev., 103, 4605-4638, https://doi.org/10.1021/cr0206420, 2003.

Balkanski, Y. J., Jacob, D. J., Gardner, G. M., Graustein, W. C., and Turekian, K. K.: Transport and residence times of tropospheric aerosols inferred from a global three-dimensional simulation of 210Pb, J. Geophys. Res.-Atmos., 98, 20573-20586, https://doi.org/10.1029/93JD02456, 1993.

Barsanti, K. C., Carlton, A. G., and Chung, S. H.: Analyzing experimental data and model parameters: implications for predictions of SOA using chemical transport models, Atmos. Chem. Phys., 13, 12073-12088, https://doi.org/10.5194/acp-13-12073-2013, 2013.

Bateman, A. P., Bertram, A. K., and Martin, S. T.: Hygroscopic Influence on the Semisolid-to-Liquid Transition of Secondary Organic Materials, J. Phys. Chem. A, 119, 4386-4395, https://doi.org/10.1021/jp508521c, 2015.

Bloss, C., Wagner, V., Jenkin, M. E., Volkamer, R., Bloss, W. J., Lee, J. D., Heard, D. E., Wirtz, K., Martin-Reviejo, M., Rea, G., Wenger, J. C., and Pilling, M. J.: Development of a detailed chemical mechanism (MCMv3.1) for the atmospheric oxidation of aromatic hydrocarbons, Atmos. Chem. Phys., 5, 641-664, https://doi.org/10.5194/acp-5-641-2005, 2005.

Calvert, J. G., Atkinson, R., Becker, K. H., Kamens, R. M., Seinfeld, J. H., Wallington, T. H., and Yarwood, G.: The Mechanisms of Atmospheric Oxidation of the Aromatic Hydrocarbons, Oxford University Press, New York, 556 pp., 2002.

Chen, Q., Heald, C. L., Jimenez, J. L., Canagaratna, M. R., Zhang, Q., He, L.-Y., Huang, X.-F., Campuzano-Jost, P., Palm, B. B., Poulain, L., Kuwata, M., Martin, S. T., Abbatt, J. P. D., Lee, A. K. Y., and Liggio, J.: Elemental composition of organic aerosol: The gap between ambient and laboratory measurements, Geophys. Res. Lett., 42, 2015GL063693, https://doi.org/10.1002/2015GL063693, 2015.

de Gouw, J. A., Middlebrook, A. M., Warneke, C., Goldan, P. D., Kuster, W. C., Roberts, J. M., Fehsenfeld, F. C., Worsnop, D. R., Canagaratna, M. R., Pszenny, A. A. P., Keene, W. C., Marchewka, M., Bertman, S. B., and Bates, T. S.: Budget of organic carbon in a polluted atmosphere: Results from the New England Air Quality Study in 2002, J. Geophys. Res.-Atmos., 110, D16305, https://doi.org/10.1029/2004JD005623, 2005.

DeCarlo, P. F., Kimmel, J. R., Trimborn, A., Northway, M. J., Jayne, J. T., Aiken, A. C., Gonin, M., Fuhrer, K., Horvath, T., Docherty, K. S., Worsnop, D. R., and Jimenez, J. L.: Field-Deployable, High-Resolution, Time-of-Flight Aerosol Mass Spectrometer, Anal. Chem., 78, 8281-8289, https://doi.org/10.1021/ac061249n, 2006.

DeCarlo, P. F., Dunlea, E. J., Kimmel, J. R., Aiken, A. C., Sueper, D., Crounse, J., Wennberg, P. O., Emmons, L., Shinozuka, Y., Clarke, A., Zhou, J., Tomlinson, J., Collins, D. R., Knapp, D., Weinheimer, A. J., Montzka, D. D., Campos, T., and Jimenez, J. L.: Fast airborne aerosol size and chemistry measurements above Mexico City and Central Mexico during the MILAGRO campaign, Atmos. Chem. Phys., 8, 4027-4048, https://doi.org/10.5194/acp-8-4027-2008, 2008.

Ding, X., Wang, X.-M., Gao, B., Fu, X.-X., He, Q.-F., Zhao, X.-Y., Yu, J.-Z., and Zheng, M.: Tracer-based estimation of secondary organic carbon in the Pearl River Delta, south China, J. Geophys. Res.-Atmos., 117, D05313, https://doi.org/10.1029/2011JD016596, 2012.

Donahue, N. M., Robinson, A. L., Stanier, C. O., and Pandis, S. N.: Coupled Partitioning, Dilution, and Chemical Aging of Semivolatile Organics, Environ. Sci. Technol., 40, 2635-2643, https://doi.org/10.1021/es052297c, 2006.

Edney, E. O., Driscoll, D. J., Speer, R. E., Weathers, W. S., Kleindienst, T. E., Li, W., and Smith, D. F.: Impact of aerosol liquid water on secondary organic aerosol yields of irradiated toluene/propylene/NOx/(NH4)2SO4/air mixtures, Atmos. Environ., 34, 3907-3919, 2000.

Ervens, B., Turpin, B. J., and Weber, R. J.: Secondary organic aerosol formation in cloud droplets and aqueous particles (aqSOA): a review of laboratory, field and model studies, Atmos. Chem. Phys., 11, 11069-11102, https://doi.org/10.5194/acp-11-11069-2011, 2011.

Faust, J. A., Wong, J. P. S., Lee, A. K. Y., and Abbatt, J. P. D.: Role of Aerosol Liquid Water in Secondary Organic Aerosol Formation from Volatile Organic Compounds, Environ. Sci. Technol., 51, 1405-1413, https://doi.org/10.1021/acs.est.6b04700, 2017.

Fisseha, R., Dommen, J., Sax, M., Paulsen, D., Kalberer, M., Maurer, R., Höfler, F., Weingartner, E., and Baltensperger, U.: Identification of Organic Acids in Secondary Organic Aerosol and the Corresponding Gas Phase from Chamber Experiments, Anal. Chem., 76, 6535-6540, https://doi.org/10.1021/ac048975f, 2004.

George, I. J., and Abbatt, J. P. D.: Heterogeneous oxidation of atmospheric aerosol particles by gas-phase radicals, Nat. Chem., 2, 713-722, 2010.

Guo, H., Xu, L., Bougiatioti, A., Cerully, K. M., Capps, S. L., Hite Jr, J. R., Carlton, A. G., Lee, S. H., Bergin, M. H., Ng, N. L., Nenes, A., and Weber, R. J.: Fine-particle water and pH in the southeastern United States, Atmos. Chem. Phys., 15, 5211-5228, https://doi.org/10.5194/acp-15-5211-2015, 2015.

Hallquist, M., Wenger, J. C., Baltensperger, U., Rudich, Y., Simpson, D., Claeys, M., Dommen, J., Donahue, N. M., George, C., Goldstein, A. H., Hamilton, J. F., Herrmann, H., Hoffmann, T., Iinuma, Y., Jang, M., Jenkin, M. E., Jimenez, J. L., Kiendler-Scharr, A., Maenhaut, W., McFiggans, G., Mentel, T. F., Monod, A., Prévôt, A. S. H., Seinfeld, J. H., Surratt, J. D., Szmigielski, R., and Wildt, J.: The formation, properties and impact of secondary organic aerosol: current and emerging

issues, Atmos. Chem. Phys., 9, 5155-5236, https://doi.org/10.5194/acp-9-5155-2009, 2009.

Hamilton, J. F., Webb, P. J., Lewis, A. C., and Reviejo, M. M.: Quantifying small molecules in secondary organic aerosol formed during the photo-oxidation of toluene with hydroxyl radicals, Atmos. Environ., 39, 7263-7275, http://dx.doi.org/10.1016/j.atmosenv.2005.09.006, 2005.

Hayes, P. L., Carlton, A. G., Baker, K. R., Ahmadov, R., Washenfelder, R. A., Alvarez, S., Rappenglück, B., Gilman, J. B., Kuster, W. C., de Gouw, J. A., Zotter, P., Prévôt, A. S. H., Szidat, S., Kleindienst, T. E., Offenberg, J. H., Ma, P. K., and Jimenez, J. L.: Modeling the formation and aging of secondary organic aerosols in Los Angeles during CalNex 2010, Atmos. Chem. Phys., 15, 5773-5801, https://doi.org/10.5194/acp-15-5773-2015, 2015.Heald, C. L., Kroll, J. H., Jimenez, J. L., Docherty, K. S., DeCarlo, P. F., Aiken, A. C., Chen, Q., Martin, S. T., Farmer, D. K., and Artaxo, P.: A simplified description of the evolution of organic aerosol composition in the atmosphere, Geophys. Res. Lett., 37, L08803, https://doi.org/10.1029/2010gl042737, 2010.

Hennigan, C. J., Bergin, M. H., Dibb, J. E., and Weber, R. J.: Enhanced secondary organic aerosol formation due to water uptake by fine particles, Geophys. Res. Lett., 35, L18801, https://doi.org/10.1029/2008GL035046, 2008.

Hildebrandt, L., Donahue, N. M., and Pandis, S. N.: High formation of secondary organic aerosol from the photo-oxidation of toluene, Atmos. Chem. Phys., 9, 2973-2986, https://doi.org/10.5194/acp-9-2973-2009, 2009.

Hodzic, A., Jimenez, J. L., Madronich, S., Canagaratna, M. R., DeCarlo, P. F., Kleinman, L., and Fast, J.: Modeling organic aerosols in a megacity: potential contribution of semi-volatile and intermediate volatility primary organic compounds to secondary organic aerosol formation, Atmos. Chem. Phys., 10, 5491-5514, https://doi.org/10.5194/acp-10-5491-2010, 2010.

Huang, D. D., Zhang, X., Dalleska, N. F., Lignell, H., Coggon, M. M., Chan, C.-M., Flagan, R. C., Seinfeld, J. H., and Chan, C. K.: A note on the effects of inorganic seed aerosol on the oxidation state of secondary organic aerosol—α-Pinene ozonolysis, J. Geophys. Res.-Atmos., 121, 2016JD025999, https://doi.org/10.1002/2016JD025999, 2016.

Ip, H. S. S., Huang, X. H. H., and Yu, J. Z.: Effective Henry's law constants of glyoxal, glyoxylic acid, and glycolic acid, Geophys. Res. Lett., 36, L01802, https://doi.org/10.1029/2008GL036212, 2009.

Jenkin, M. E., Saunders, S. M., Wagner, V., and Pilling, M. J.: Protocol for the development of the Master Chemical Mechanism, MCM v3 (Part B): tropospheric degradation of aromatic volatile organic compounds, Atmos. Chem. Phys., 3, 181-193, https://doi.org/10.5194/acp-3-181-2003, 2003.

Kamens, R. M., Zhang, H. F., Chen, E. H., Zhou, Y., Parikh, H. M., Wilson, R. L., Galloway, K. E., and Rosen, E. P.: Secondary organic aerosol formation from toluene in an atmospheric hydrocarbon mixture: Water and particle seed effects, Atmos. Environ., 45, 2324-2334, https://doi.org/doi:10.1016/j.atmosenv.2010.11.007, 2011.

572 Kampf, C. J., Waxman, E. M., Slowik, J. G., Dommen, J., Pfaffenberger, L., Praplan, A. P.,
573 Prévôt, A. S. H., Baltensperger, U., Hoffmann, T., and Volkamer, R.: Effective
574 Henry's Law Partitioning and the Salting Constant of Glyoxal in Aerosols Containing
575 Sulfate, Environ. Sci. Technol., 47, 4236-4244, https://doi.org/10.1021/es400083d,
576 2013.
577 Kang, E., Root, M. J., Toohey, D. W., and Brune, W. H.: Introducing the concept of Potential
578 Aerosol Mass (PAM), Atmos. Chem. Phys., 7, 5727-5744,
579 https://doi.org/10.5194/acp-7-5727-2007, 2007.
580 Kang, E., Toohey, D. W., and Brune, W. H.: Dependence of SOA oxidation on organic
581 aerosol mass concentration and OH exposure: experimental PAM chamber studies,
582 Atmos. Chem. Phys., 11, 1837-1852, https://doi.org/10.5194/acp-11-1837-2011,
583 2011.
584 Krechmer, J. E., Pagonis, D., Ziemann, P. J., and Jimenez, J. L.: Quantification of Gas-Wall
585 Partitioning in Teflon Environmental Chambers Using Rapid Bursts of Low-
586 Volatility Oxidized Species Generated in Situ, Environ. Sci. Technol., 50, 5757-5765,
587 https://doi.org/10.1021/acs.est.6b00606, 2016.
588 Kreidenweis, S. M., Petters, M. D., and DeMott, P. J.: Single-parameter estimates of
589 aerosol water content, Environ. Res. Lett., 3, 035002, 2008.
590 Kroll, J. H., Smith, J. D., Che, D. L., Kessler, S. H., Worsnop, D. R., and Wilson, K. R.:
591 Measurement of fragmentation and functionalization pathways in the heterogeneous
592 oxidation of oxidized organic aerosol, Phys. Chem. Chem. Phys., 11, 8005-8014,
593 https://doi.org/10.1039/B905289E, 2009.
594 Kroll, J. H., Donahue, N. M., Jimenez, J. L., Kessler, S. H., Canagaratna, M. R., Wilson, K.
595 R., Altieri, K. E., Mazzoleni, L. R., Wozniak, A. S., Bluhm, H., Mysak, E. R., Smith,
596 J. D., Kolb, C. E., and Worsnop, D. R.: Carbon oxidation state as a metric for
597 describing the chemistry of atmospheric organic aerosol, Nat. Chem., 3, 133-139,
598 2011.
599 Lambe, A. T., Ahern, A. T., Williams, L. R., Slowik, J. G., Wong, J. P. S., Abbatt, J. P. D.,
600 Brune, W. H., Ng, N. L., Wright, J. P., Croasdale, D. R., Worsnop, D. R., Davidovits,
601 P., and Onasch, T. B.: Characterization of aerosol photooxidation flow reactors:
602 heterogeneous oxidation, secondary organic aerosol formation and cloud
603 condensation nuclei activity measurements, Atmos. Meas. Tech., 4, 445-461,
604 https://doi.org/10.5194/amt-4-445-2011, 2011a.
605 Lambe, A. T., Onasch, T. B., Massoli, P., Croasdale, D. R., Wright, J. P., Ahern, A. T.,
606 Williams, L. R., Worsnop, D. R., Brune, W. H., and Davidovits, P.: Laboratory
607 studies of the chemical composition and cloud condensation nuclei (CCN) activity of
608 secondary organic aerosol (SOA) and oxidized primary organic aerosol (OPOA),
609 Atmos. Chem. Phys., 11, 8913-8928, https://doi.org/10.5194/acp-11-8913-2011,
610 2011b.
611 Lambe, A. T., Chhabra, P. S., Onasch, T. B., Brune, W. H., Hunter, J. F., Kroll, J. H.,
612 Cummings, M. J., Brogan, J. F., Parmar, Y., Worsnop, D. R., Kolb, C. E., and
613 Davidovits, P.: Effect of oxidant concentration, exposure time, and seed particles on
614 secondary organic aerosol chemical composition and yield, Atmos. Chem. Phys., 15,
615 3063-3075, https://doi.org/10.5194/acp-15-3063-2015, 2015.

Lee, A. K. Y., Herckes, P., Leaitch, W. R., Macdonald, A. M., and Abbatt, J. P. D.: Aqueous OH oxidation of ambient organic aerosol and cloud water organics: Formation of highly oxidized products, Geophys. Res. Lett., 38, L11805, https://doi.org/10.1029/2011GL047439, 2011.

Lee, Y. H., and Adams, P. J.: Evaluation of aerosol distributions in the GISS-TOMAS global aerosol microphysics model with remote sensing observations, Atmos. Chem. Phys., 10, 2129-2144, https://doi.org/10.5194/acp-10-2129-2010, 2010.

Liao, H., and Seinfeld, J. H.: Global impacts of gas-phase chemistry-aerosol interactions on direct radiative forcing by anthropogenic aerosols and ozone, J. Geophys. Res.-Atmos., 110, D18208, https://doi.org/10.1029/2005JD005907, 2005.

Liggio, J., Li, S.-M., and McLaren, R.: Heterogeneous Reactions of Glyoxal on Particulate Matter: Identification of Acetals and Sulfate Esters, Environ. Sci. Technol., 39, 1532-1541, https://doi.org/10.1021/es048375y, 2005a.

Liggio, J., Li, S.-M., and McLaren, R.: Reactive uptake of glyoxal by particulate matter, J. Geophys. Res.-Atmos., 110, D10304, https://doi.org/10.1029/2004JD005113, 2005b.

Lim, Y. B., Tan, Y., Perri, M. J., Seitzinger, S. P., and Turpin, B. J.: Aqueous chemistry and its role in secondary organic aerosol (SOA) formation, Atmos. Chem. Phys., 10, 10521-10539, https://doi.org/10.5194/acp-10-10521-2010, 2010.

Liu, T., Li, Z., Chan, M., and Chan, C. K.: Formation of secondary organic aerosols from gas-phase emissions of heated cooking oils, Atmos. Chem. Phys., 17, 7333-7344, https://doi.org/10.5194/acp-17-7333-2017, 2017.

Ma, P. K., Zhao, Y., Robinson, A. L., Worton, D. R., Goldstein, A. H., Ortega, A. M., Jimenez, J. L., Zotter, P., Prévôt, A. S. H., Szidat, S., and Hayes, P. L.: Evaluating the impact of new observational constraints on P-S/IVOC emissions, multi-generation oxidation, and chamber wall losses on SOA modeling for Los Angeles, CA, Atmos. Chem. Phys., 17, 9237-9259, https://doi.org/10.5194/acp-17-9237-2017, 2017.

Mahmud, A., and Barsanti, K.: Improving the representation of secondary organic aerosol (SOA) in the MOZART-4 global chemical transport model, Geosci. Model Dev., 6, 961-980, 10.5194/gmd-6-961-2013, 2013.

Mao, J., Ren, X., Brune, W. H., Olson, J. R., Crawford, J. H., Fried, A., Huey, L. G., Cohen, R. C., Heikes, B., Singh, H. B., Blake, D. R., Sachse, G. W., Diskin, G. S., Hall, S. R., and Shetter, R. E.: Airborne measurement of OH reactivity during INTEX-B, Atmos. Chem. Phys., 9, 163-173, https://doi.org/10.5194/acp-9-163-2009, 2009.

Matsunaga, A., and Ziemann ‡, P. J.: Gas-Wall Partitioning of Organic Compounds in a Teflon Film Chamber and Potential Effects on Reaction Product and Aerosol Yield Measurements, Aerosol Sci. Tech., 44, 881-892, https://doi.org/10.1080/02786826.2010.501044, 2010.

Matthew, B. M., Middlebrook, A. M., and Onasch, T. B.: Collection Efficiencies in an Aerodyne Aerosol Mass Spectrometer as a Function of Particle Phase for Laboratory Generated Aerosols, Aerosol Sci. Tech., 42, 884-898, https://doi.org/10.1080/02786820802356797, 2008.

Middlebrook, A. M., Bahreini, R., Jimenez, J. L., and Canagaratna, M. R.: Evaluation of Composition-Dependent Collection Efficiencies for the Aerodyne Aerosol Mass

Spectrometer using Field Data, Aerosol Sci. Tech., 46, 258-271, https://doi.org/10.1080/02786826.2011.620041, 2012.

Ng, N. L., Kroll, J. H., Chan, A. W. H., Chhabra, P. S., Flagan, R. C., and Seinfeld, J. H.: Secondary organic aerosol formation from m-xylene, toluene, and benzene, Atmos. Chem. Phys., 7, 3909-3922, https://doi.org/10.5194/acp-7-3909-2007, 2007.

Ng, N. L., Canagaratna, M. R., Zhang, Q., Jimenez, J. L., Tian, J., Ulbrich, I. M., Kroll, J. H., Docherty, K. S., Chhabra, P. S., Bahreini, R., Murphy, S. M., Seinfeld, J. H., Hildebrandt, L., Donahue, N. M., DeCarlo, P. F., Lanz, V. A., Prévôt, A. S. H., Dinar, E., Rudich, Y., and Worsnop, D. R.: Organic aerosol components observed in Northern Hemispheric datasets from Aerosol Mass Spectrometry, Atmos. Chem. Phys., 10, 4625-4641, https://doi.org/10.5194/acp-10-4625-2010, 2010.

Ng, N. L., Canagaratna, M. R., Jimenez, J. L., Chhabra, P. S., Seinfeld, J. H., and Worsnop, D. R.: Changes in organic aerosol composition with aging inferred from aerosol mass spectra, Atmos. Chem. Phys., 11, 6465-6474, https://doi.org/10.5194/acp-11-6465-2011, 2011.

Nguyen, T. K. V., Zhang, Q., Jimenez, J. L., Pike, M., and Carlton, A. G.: Liquid Water: Ubiquitous Contributor to Aerosol Mass, Environ. Sci. Technol. Lett., 3, 257-263, https://doi.org/10.1021/acs.estlett.6b00167, 2016.

Ortega, A. M., Hayes, P. L., Peng, Z., Palm, B. B., Hu, W., Day, D. A., Li, R., Cubison, M. J., Brune, W. H., Graus, M., Warneke, C., Gilman, J. B., Kuster, W. C., de Gouw, J., Gutiérrez-Montes, C., and Jimenez, J. L.: Real-time measurements of secondary organic aerosol formation and aging from ambient air in an oxidation flow reactor in the Los Angeles area, Atmos. Chem. Phys., 16, 7411-7433, https://doi.org/10.5194/acp-16-7411-2016, 2016.

Palm, B. B., Campuzano-Jost, P., Ortega, A. M., Day, D. A., Kaser, L., Jud, W., Karl, T., Hansel, A., Hunter, J. F., Cross, E. S., Kroll, J. H., Peng, Z., Brune, W. H., and Jimenez, J. L.: In situ secondary organic aerosol formation from ambient pine forest air using an oxidation flow reactor, Atmos. Chem. Phys., 16, 2943-2970, https://doi.org/10.5194/acp-16-2943-2016, 2016.

Parikh, H. M., Carlton, A. G., Vizuete, W., and Kamens, R. M.: Modeling secondary organic aerosol using a dynamic partitioning approach incorporating particle aqueous-phase chemistry, Atmos. Environ., 45, 1126-1137, http://dx.doi.org/10.1016/j.atmosenv.2010.11.027, 2011.

Peng, Z., Day, D. A., Ortega, A. M., Palm, B. B., Hu, W., Stark, H., Li, R., Tsigaridis, K., Brune, W. H., and Jimenez, J. L.: Non-OH chemistry in oxidation flow reactors for the study of atmospheric chemistry systematically examined by modeling, Atmos. Chem. Phys., 16, 4283-4305, https://doi.org/10.5194/acp-16-4283-2016, 2016.

Peng, Z., and Jimenez, J. L.: Modeling of the chemistry in oxidation flow reactors with high initial NO, Atmos. Chem. Phys., 17, 11991-12010, https://doi.org/10.5194/acp-17-11991-2017, 2017.

Romonosky, D. E., Laskin, A., Laskin, J., and Nizkorodov, S. A.: High-Resolution Mass Spectrometry and Molecular Characterization of Aqueous Photochemistry Products of Common Types of Secondary Organic Aerosols, The Journal of Physical Chemistry A, 119, 2594-2606, https://doi.org/10.1021/jp509476r, 2015.

Rudich, Y., Donahue, N. M., and Mentel, T. F.: Aging of organic aerosol: Bridging the gap between laboratory and field studies, Annual Review of Physical Chemistry, 58, 321-352, https://doi.org/10.1146/annurev.physchem.58.032806.104432, 2007.

Ruehl, C. R., Nah, T., Isaacman, G., Worton, D. R., Chan, A. W. H., Kolesar, K. R., Cappa, C. D., Goldstein, A. H., and Wilson, K. R.: The Influence of Molecular Structure and Aerosol Phase on the Heterogeneous Oxidation of Normal and Branched Alkanes by OH, J. Phys. Chem. A, 117, 3990-4000, https://doi.org/10.1021/jp401888q, 2013.

Sareen, N., Waxman, E. M., Turpin, B. J., Volkamer, R., and Carlton, A. G.: Potential of Aerosol Liquid Water to Facilitate Organic Aerosol Formation: Assessing Knowledge Gaps about Precursors and Partitioning, Environ. Sci. Technol., 51, 3327-3335, https://doi.org/10.1021/acs.est.6b04540, 2017.

Sato, K., Hatakeyama, S., and Imamura, T.: Secondary organic aerosol formation during the photooxidation of toluene: NOx dependence of chemical composition, J. Phys. Chem. A, 111, 9796-9808, https://doi.org/10.1021/jp071419f, 2007.

Seinfeld, J. H.; Pandis, S. N. Atmospheric Chemistry and Physics:From Air Pollution to Climate Change, 2nd ed.; Wiley: Hoboken, NJ, 2006.

Shrivastava, M., Fast, J., Easter, R., Gustafson Jr, W. I., Zaveri, R. A., Jimenez, J. L., Saide, P., and Hodzic, A.: Modeling organic aerosols in a megacity: comparison of simple and complex representations of the volatility basis set approach, Atmos. Chem. Phys., 11, 6639-6662, https://doi.org/10.5194/acp-11-6639-2011, 2011.

Smith, M. L., Kuwata, M., and Martin, S. T.: Secondary Organic Material Produced by the Dark Ozonolysis of α-Pinene Minimally Affects the Deliquescence and Efflorescence of Ammonium Sulfate, Aerosol Sci. Tech., 45, 244-261, https://doi.org/10.1080/02786826.2010.532178, 2011.

Smith, M. L., Bertram, A. K., and Martin, S. T.: Deliquescence, efflorescence, and phase miscibility of mixed particles of ammonium sulfate and isoprene-derived secondary organic material, Atmos. Chem. Phys., 12, 9613-9628, https://doi.org/10.5194/acp-12-9613-2012, 2012.

Smith, M. L., You, Y., Kuwata, M., Bertram, A. K., and Martin, S. T.: Phase Transitions and Phase Miscibility of Mixed Particles of Ammonium Sulfate, Toluene-Derived Secondary Organic Material, and Water, J. Phys. Chem. A, 117, 8895-8906, https://doi.org/10.1021/jp405095e, 2013.

Song, M., Liu, P. F., Hanna, S. J., Zaveri, R. A., Potter, K., You, Y., Martin, S. T., and Bertram, A. K.: Relative humidity-dependent viscosity of secondary organic material from toluene photo-oxidation and possible implications for organic particulate matter over megacities, Atmos. Chem. Phys., 16, 8817-8830, https://doi.org/10.5194/acp-16-8817-2016, 2016.

Takahama, S., Pathak, R. K., and Pandis, S. N.: Efflorescence Transitions of Ammonium Sulfate Particles Coated with Secondary Organic Aerosol, Environ. Sci. Technol., 41, 2289-2295, https://doi.org/10.1021/es0619915, 2007.

Tsigaridis, K., Daskalakis, N., Kanakidou, M., Adams, P. J., Artaxo, P., Bahadur, R., Balkanski, Y., Bauer, S. E., Bellouin, N., Benedetti, A., Bergman, T., Berntsen, T. K., Beukes, J. P., Bian, H., Carslaw, K. S., Chin, M., Curci, G., Diehl, T., Easter, R. C., Ghan, S. J., Gong, S. L., Hodzic, A., Hoyle, C. R., Iversen, T., Jathar, S., Jimenez, J.

L., Kaiser, J. W., Kirkevåg, A., Koch, D., Kokkola, H., Lee, Y. H., Lin, G., Liu, X., Luo, G., Ma, X., Mann, G. W., Mihalopoulos, N., Morcrette, J. J., Müller, J. F., Myhre, G., Myriokefalitakis, S., Ng, N. L., O'Donnell, D., Penner, J. E., Pozzoli, L., Pringle, K. J., Russell, L. M., Schulz, M., Sciare, J., Seland, Ø., Shindell, D. T., Sillman, S., Skeie, R. B., Spracklen, D., Stavrakou, T., Steenrod, S. D., Takemura, T., Tiitta, P., Tilmes, S., Tost, H., van Noije, T., van Zyl, P. G., von Salzen, K., Yu, F., Wang, Z., Wang, Z., Zaveri, R. A., Zhang, H., Zhang, K., Zhang, Q., and Zhang, X.: The AeroCom evaluation and intercomparison of organic aerosol in global models, Atmos. Chem. Phys., 14, 10845-10895, https://doi.org/10.5194/acp-14-10845-2014, 2014.

Volkamer, R., Jimenez, J. L., San Martini, F., Dzepina, K., Zhang, Q., Salcedo, D., Molina, L. T., Worsnop, D. R., and Molina, M. J.: Secondary organic aerosol formation from anthropogenic air pollution: Rapid and higher than expected, Geophys. Res. Lett., 33, L17811, https://doi.org/10.1029/2006gl026899, 2006.

Wong, J. P. S., Lee, A. K. Y., and Abbatt, J. P. D.: Impacts of Sulfate Seed Acidity and Water Content on Isoprene Secondary Organic Aerosol Formation, Environ. Sci. Technol., 49, 13215-13221, https://doi.org/10.1021/acs.est.5b02686, 2015.

Zhang, X., Cappa, C. D., Jathar, S. H., McVay, R. C., Ensberg, J. J., Kleeman, M. J., and Seinfeld, J. H.: Influence of vapor wall loss in laboratory chambers on yields of secondary organic aerosol, P. Natl. Acad. Sci., 111, 5802-5807, https://doi.org/10.1073/pnas.1404727111, 2014.

Zhang, X., Schwantes, R. H., McVay, R. C., Lignell, H., Coggon, M. M., Flagan, R. C., and Seinfeld, J. H.: Vapor wall deposition in Teflon chambers, Atmos. Chem. Phys., 15, 4197-4214, https://doi.org/10.5194/acp-15-4197-2015, 2015.

Zhang, Z., Zhang, Y., Wang, X., Lü, S., Huang, Z., Huang, X., Yang, W., Wang, Y., and Zhang, Q.: Spatiotemporal patterns and source implications of aromatic hydrocarbons at six rural sites across China's developed coastal regions, J. Geophys. Res.-Atmos., 121, 2016JD025115, https://doi.org/10.1002/2016JD025115, 2016.

Zhao, Y., Saleh, R., Saliba, G., Presto, A. A., Gordon, T. D., Drozd, G. T., Goldstein, A. H., Donahue, N. M., and Robinson, A. L.: Reducing secondary organic aerosol formation from gasoline vehicle exhaust, P. Natl. Acad. Sci., 114, 6984-6989, https://doi.org/10.1073/pnas.1620911114, 2017.

780 **Table 1.** Summary of the results for the initially dry and wet AS seeds experiments.

OH exposure ($\times 10^{11}$ molecules cm^{-3} s)	$[toluene]_{reacted}$ (ppb)	$[toluene]_{final}$ (ppb)	ε [a]	
			wet AS	dry AS
0.47	32.4	106.0	0.57	0.56
1.66	84.9	53.5	0.82	0.82
2.97	113.1	25.3	0.83	0.85
4.34	126.9	11.5	0.83	0.85
5.28	131.7	6.7	0.83	0.85

781 [a] The volume fraction of organics.

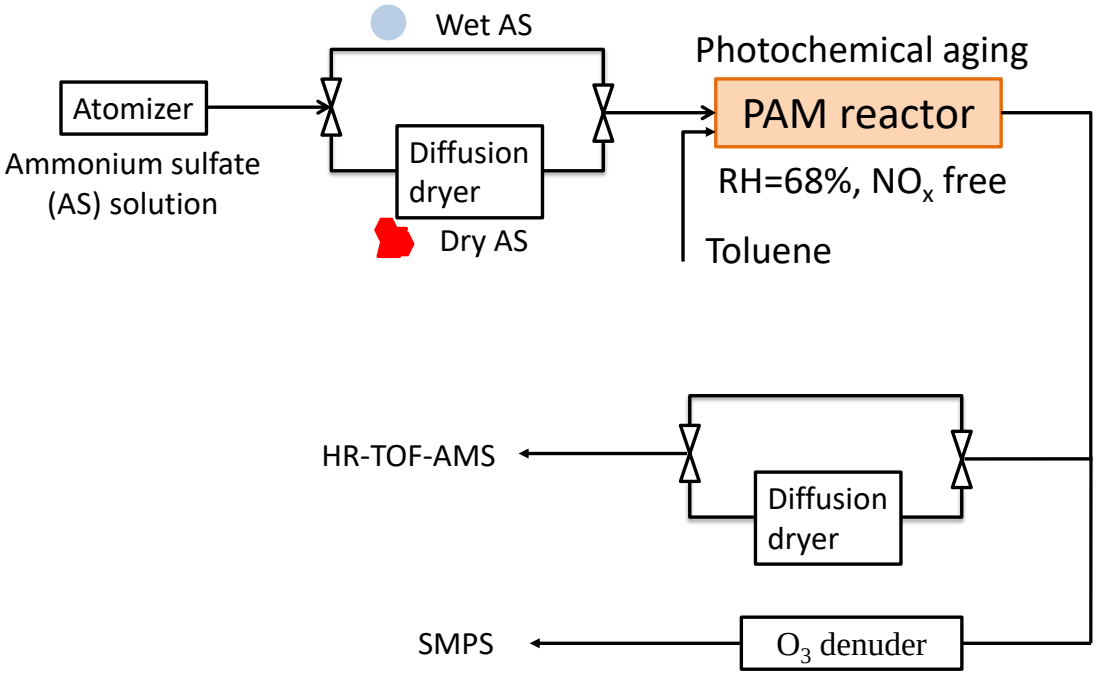

Fig. 1. Schematic of the experimental setup. The aqueous ammonium sulfate (AS) seed particles either passed through a diffusion dryer so that the phase of the seed particles could be altered or bypassed the diffusion dryer. Either wet or dry AS served as seed particles for the experiments.

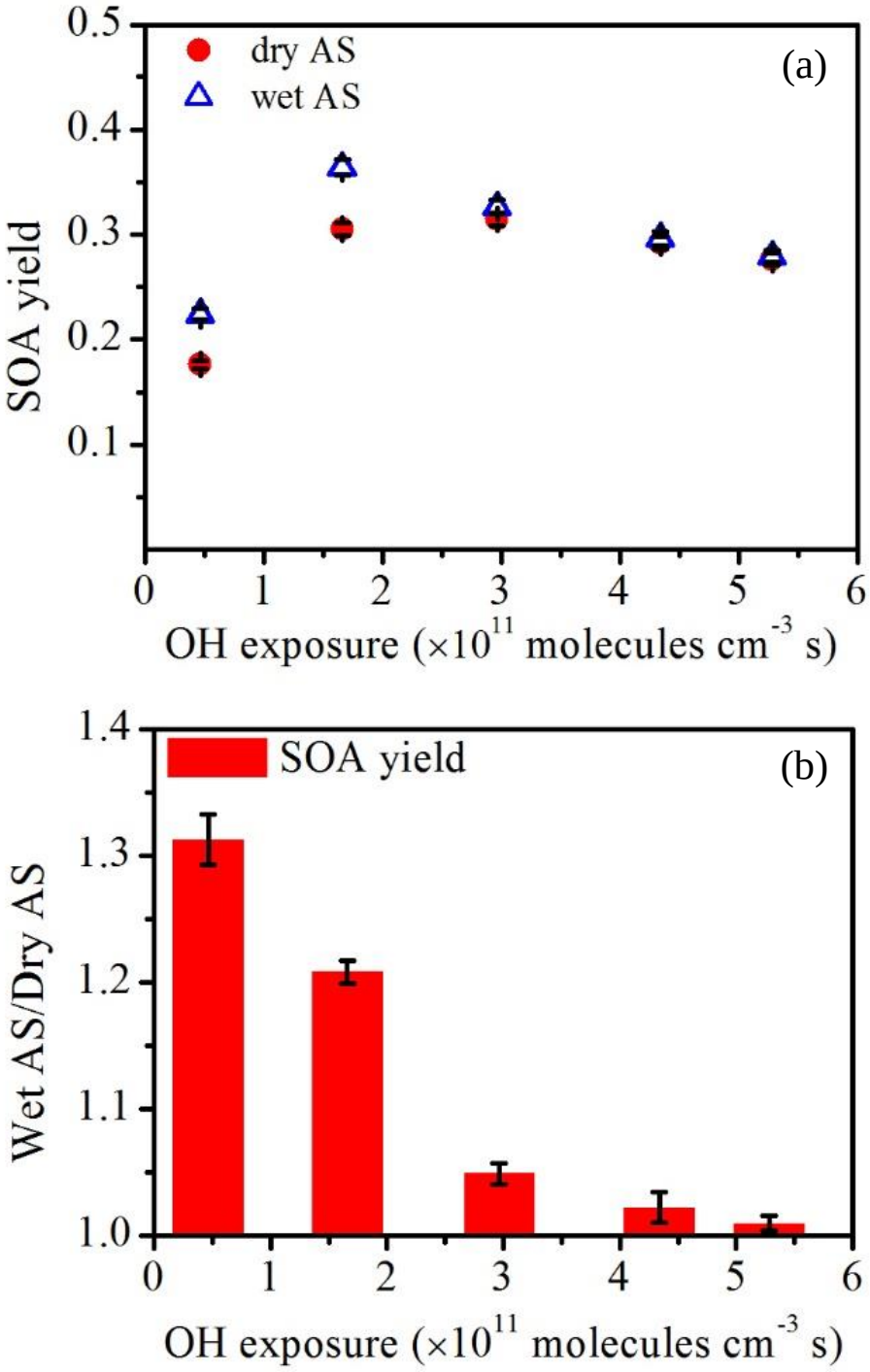

788

789 **Fig. 2.** (a) Yield of toluene-derived SOA formed on initially wet and dry AS as a

790 function of OH exposure. (b) Ratio of SOA yields on initially wet AS to those on

791 initially dry AS as a function of OH exposure.

792

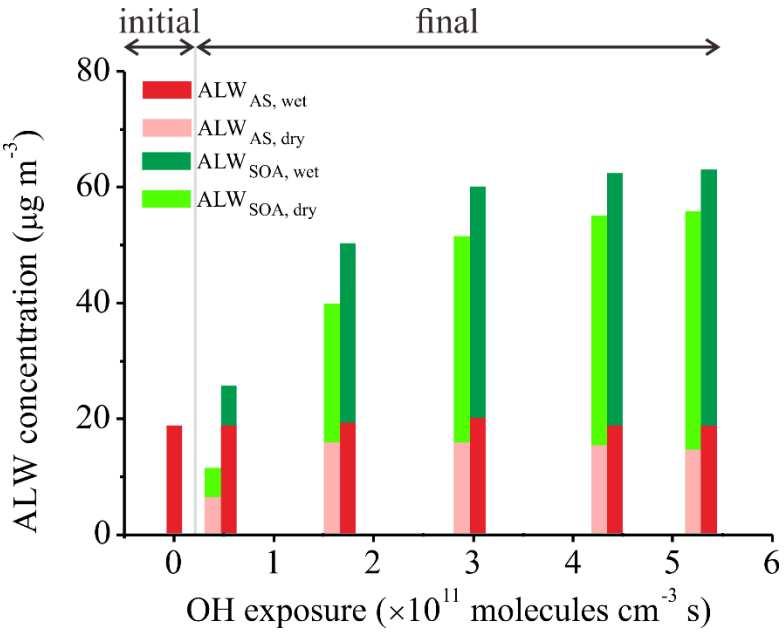

793

794 **Fig. 3.** Mass concentration of ALW uptake by AS and toluene-derived SOA before

795 (initial) and after reactions (final) for both initially wet and dry AS seeds. Adjoining

796 bars for initially wet and dry seeds have same OH exposures.

797

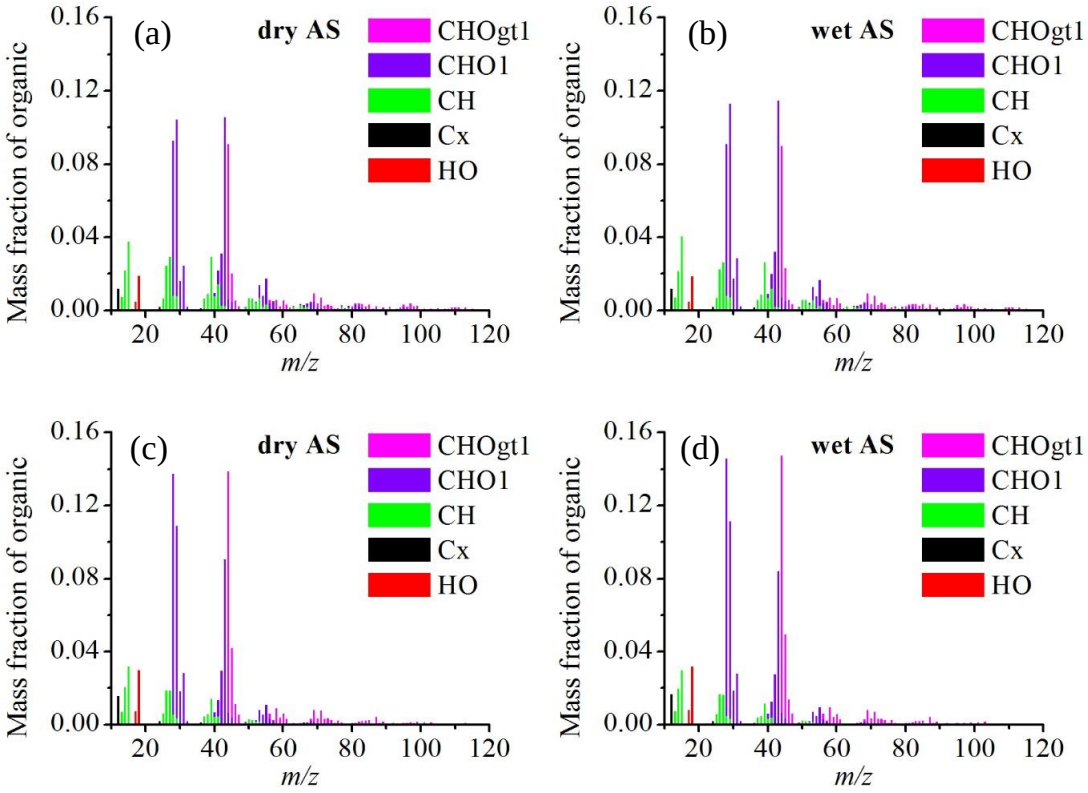

798

799 **Fig. 4.** High-resolution mass spectra of toluene-derived SOA on initially wet and dry

800 AS at an OH exposure of (a, b) 0.47×10^{11} molecules cm^{-3} s and (c, d) 5.28×10^{11}

801 molecules cm^{-3} s.

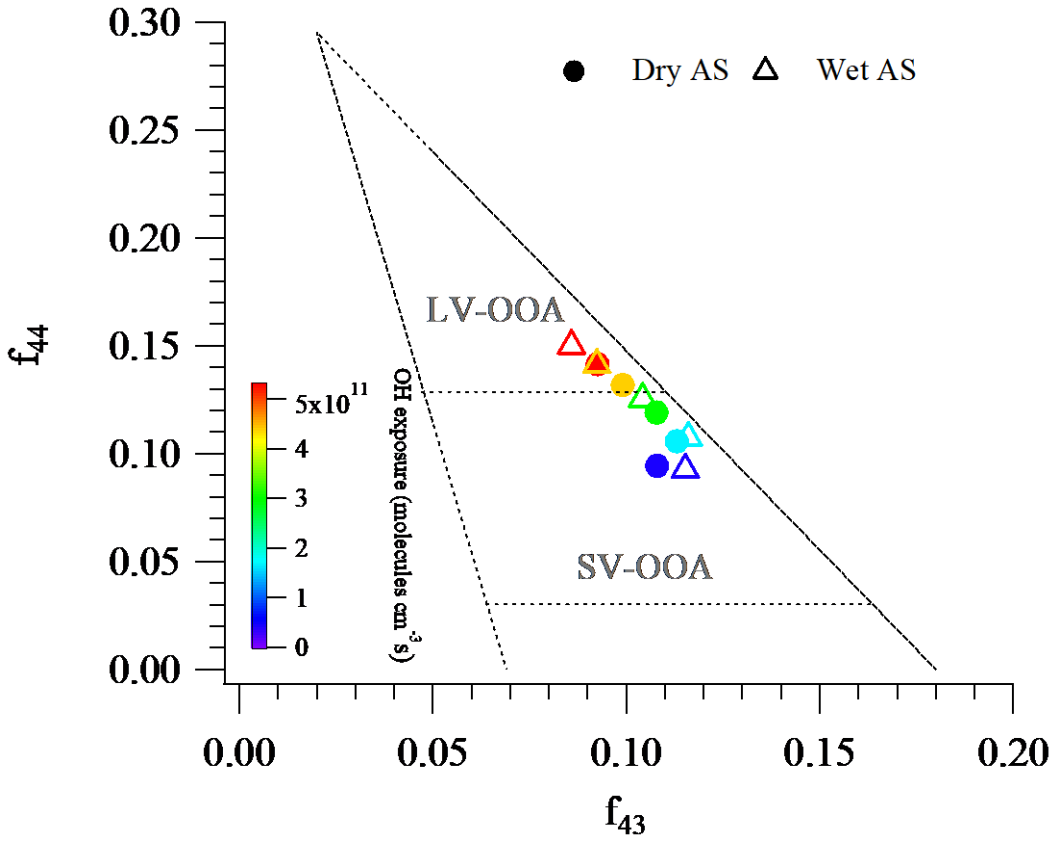

802

803 **Fig. 5.** Fractions of total organic signal at *m/z* 43 (f_{43}) vs. *m/z* 44 (f_{44}) from SOA data

804 obtained in this study together with the triangle plot of Ng et al. (2010). Ambient SV–

805 OOA and LV–OOA regions are adapted from Ng et al. (2010). Data are colored

806 according to the OH exposure.

807

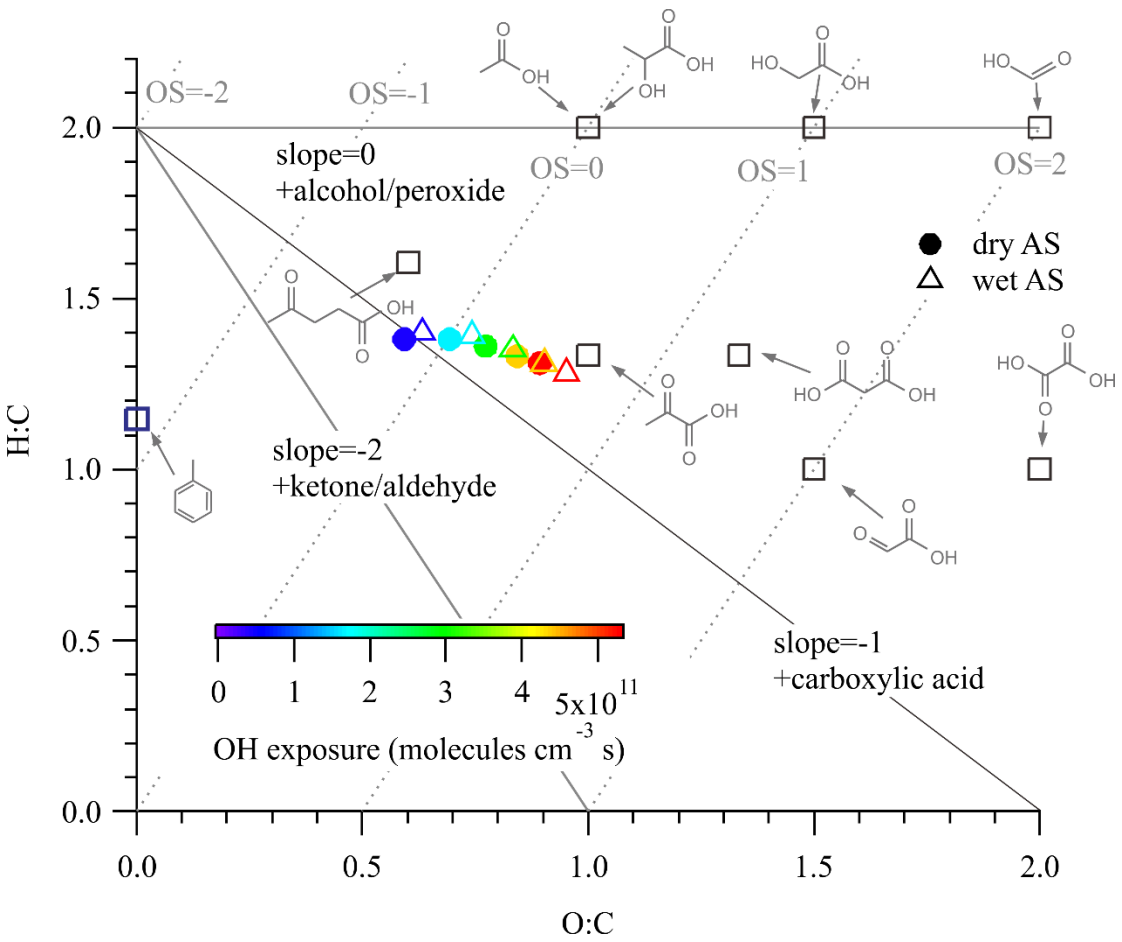

Fig. 6. Van Krevelen diagram of SOA derived from the photooxidation of toluene on initially wet and dry AS seed particles. SOA data are colored according to the OH exposure. Products identified in toluene-derived SOA are shown in boxes (Bloss et al., 2005; Hamilton et al., 2005; Sato et al., 2007). Average carbon oxidation states from Kroll et al. (2011) and functionalization slopes from Heald et al. (2010) are shown for reference.